3D hierarchical CoO@MnO_2 core-shell nanohybrid for high-energy solid state asymmetric supercapacitors

Chao Li,[a] Jayaraman Balamurugan,[a] Tran Duy Thanh,[a] Nam Hoon Kim,[a*] Joong Hee Lee [a,b*]

[a]Advanced Materials Institute of BIN Convergence Technology (BK21Plus Global) & Dept. of BIN Convergence Technology, Chonbuk National University, Jeonju, Jeonbuk, 54896, Republic of Korea.

[b]Carbon Composite Research Center, Department of Polymer-Nano Science and Technology, Chonbuk National University, Jeonju, Jeonbuk, 54896, Republic of Korea.

Corresponding to Prof. Joong Hee Lee (jhl@jbnu.ac.kr) and Prof. Nam Hoon Kim (nhk@jbnu.ac.kr)

**Corresponding author:* Fax: +82 63 270 2341; Tel: +82 63 270 2342

Email address: Prof. Joong Hee Lee (jhl@jbnu.ac.kr) and Prof. Nam Hoon Kim (nhk@jbnu.ac.kr)

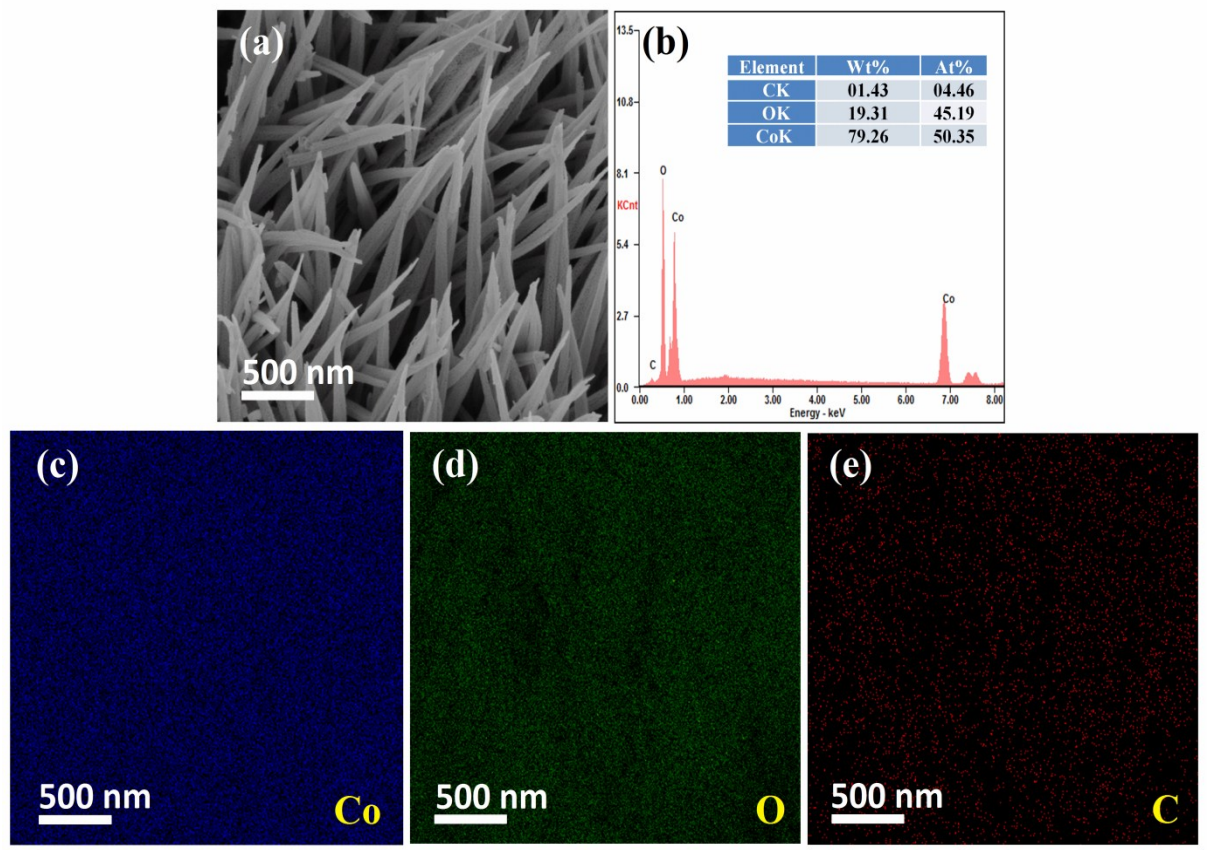

Fig. S1 (a) FE-SEM, (b) EDAX, and (c-e) EDS color mapping of the carbon coated CoO NWs/Ni foam.

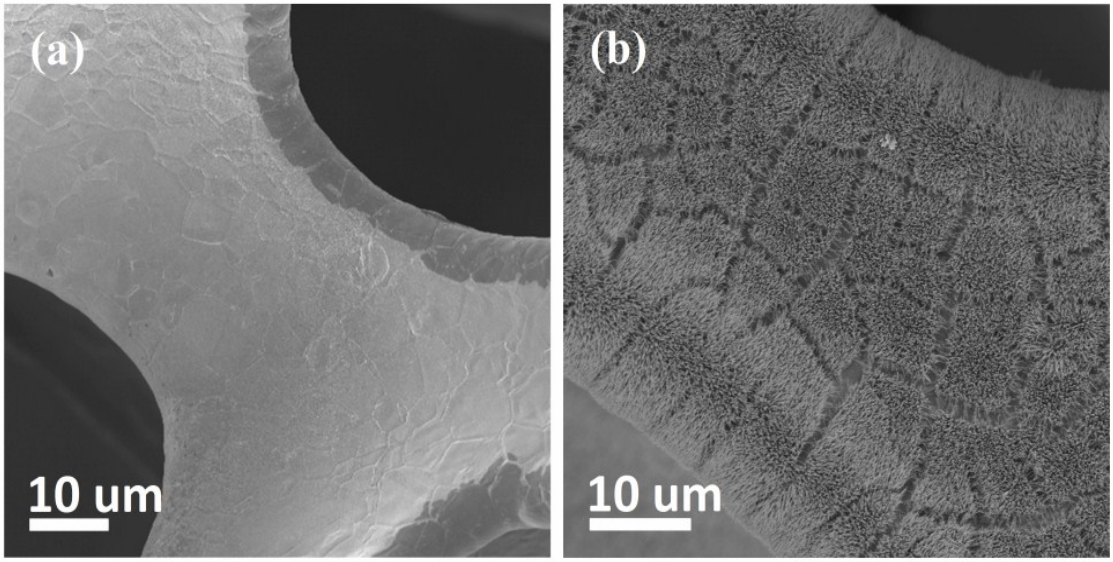

Fig. S2 FE-SEM images of (a) Bare Ni foam, and (b) as-synthesized CoO NWs/Ni foam.

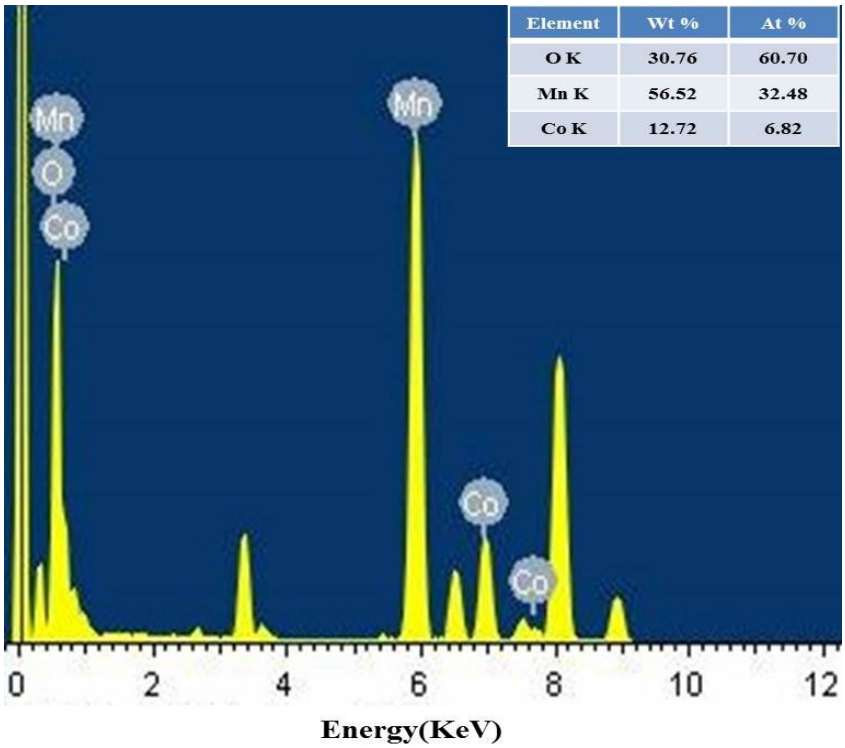

Fig. S3 EDAX spectrum of 3D CoO@MnO_2 core-shell nanohybrid.

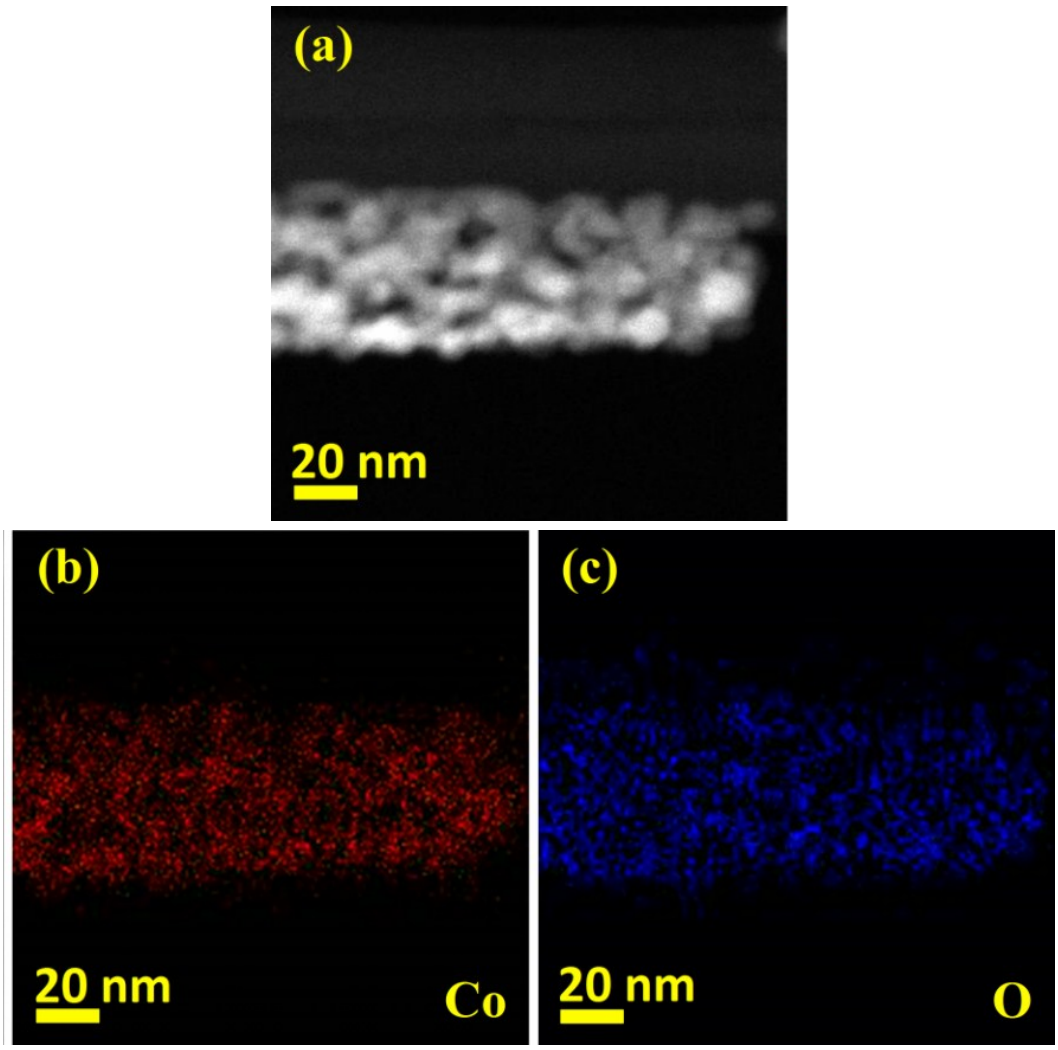

Fig. S4 Dark field STEM elemental mapping analysis of the CoO NWs (a) selected area and corresponding elemental mapping of (b) cobalt, (c) oxygen.

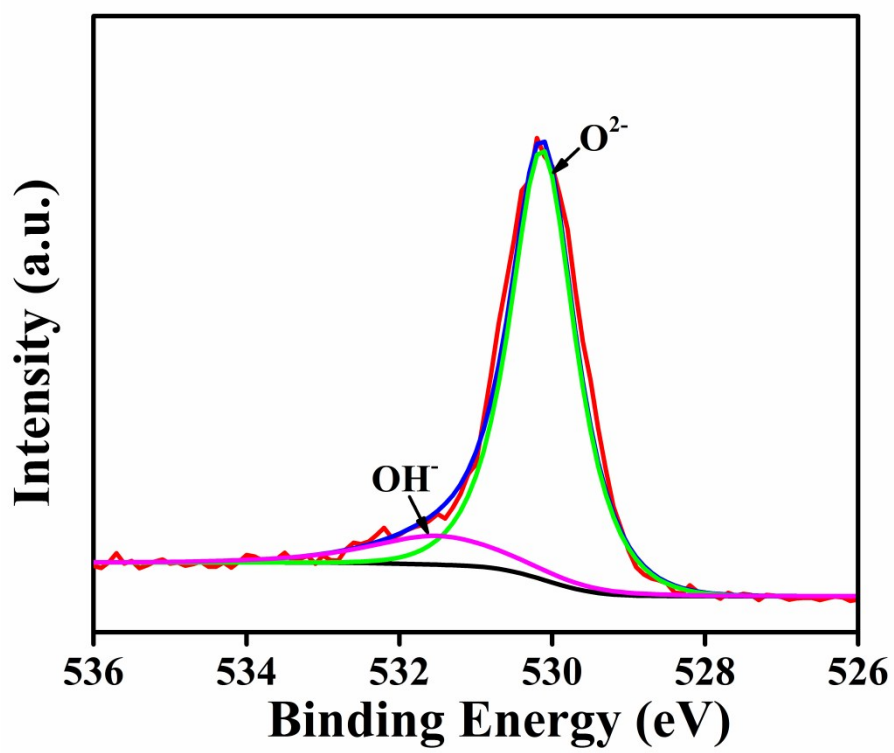

Fig. S5 High-resolution XPS spectrum of O1s for 3D CoO@MnO_2 core-shell nanohybrid.

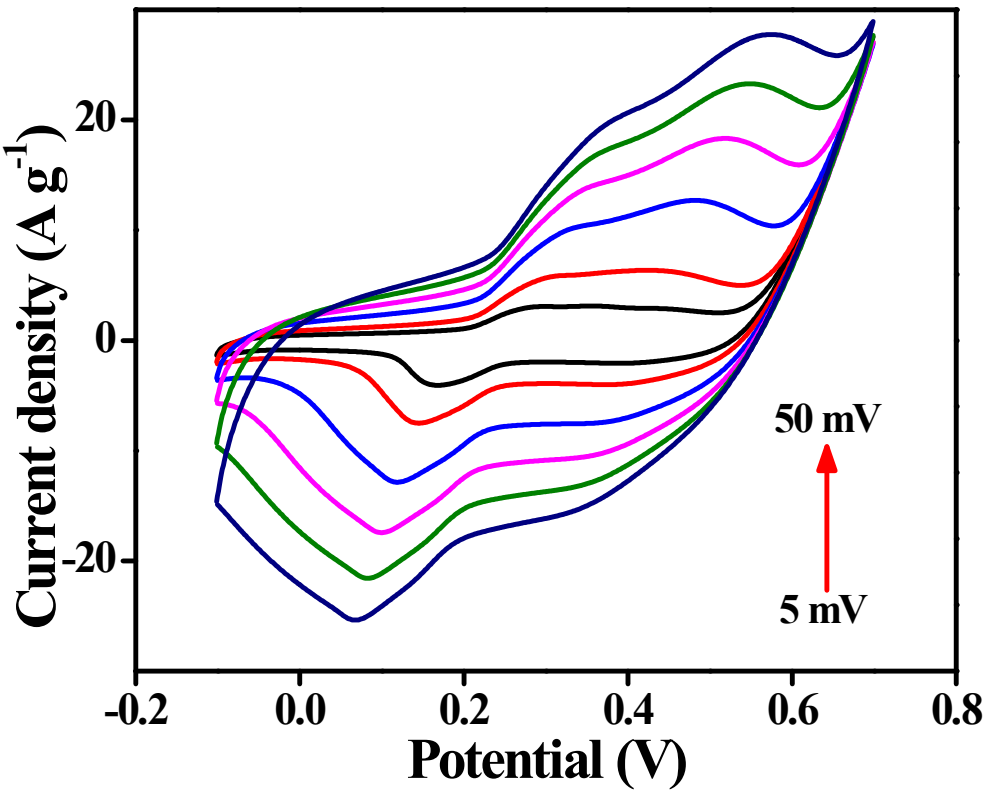

Fig. S6 CV curves with different scan rates of CoO NWs.

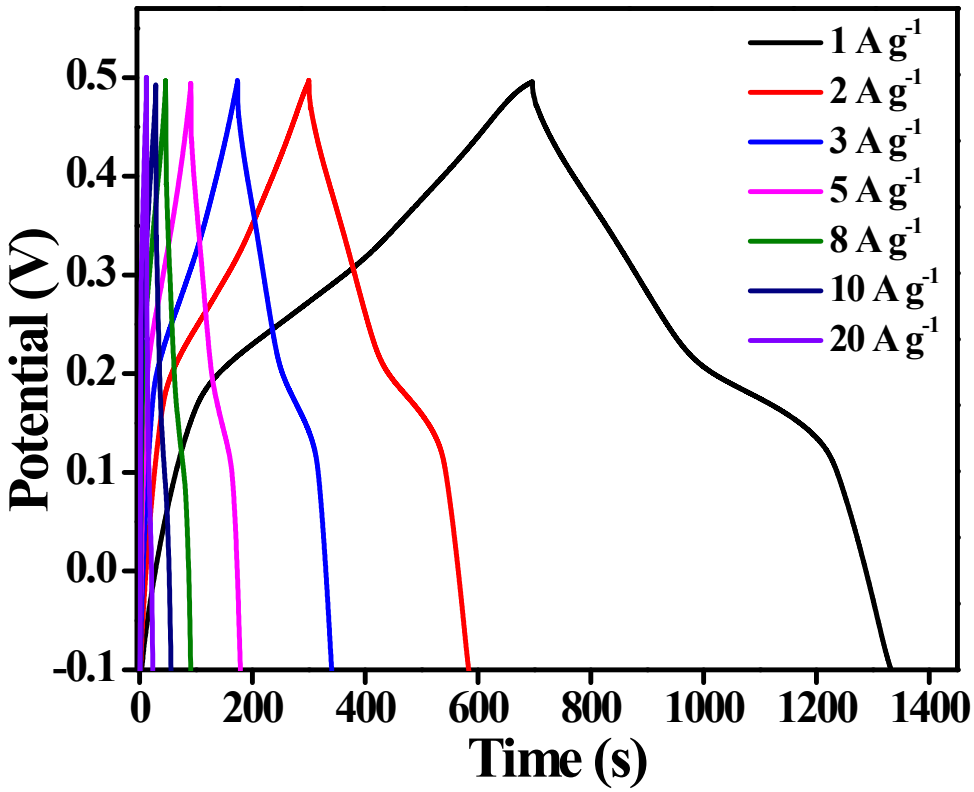

Fig. S7 GCD curves of 3 D CoO NWs at different current density.

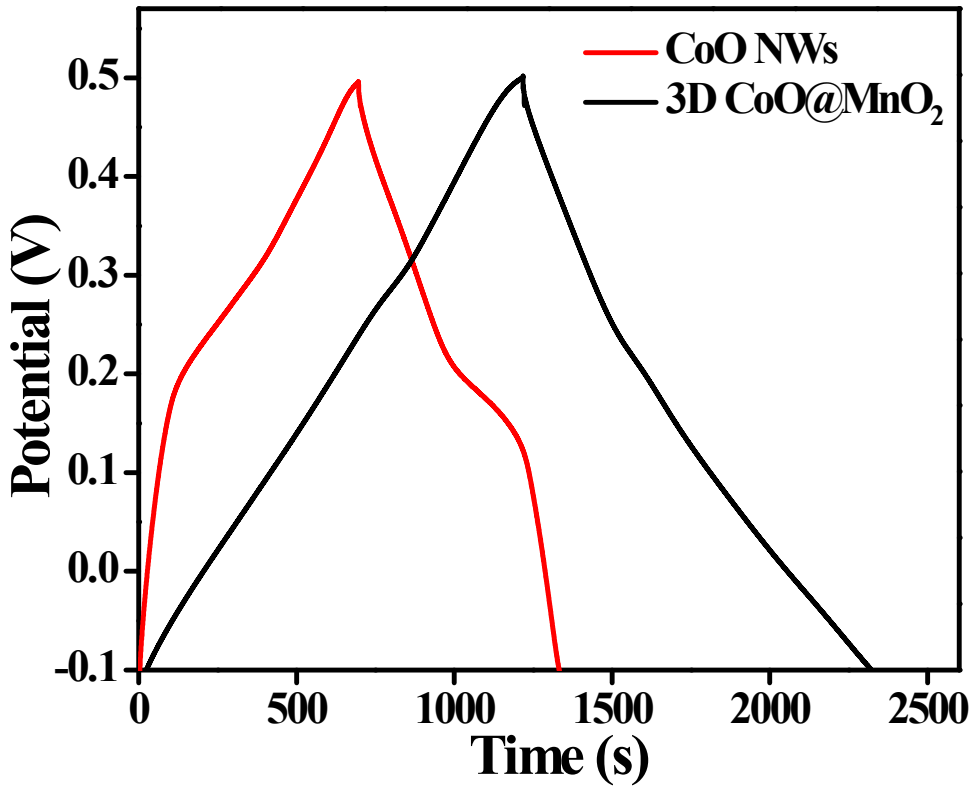

Fig. S8 GCD curves of CoO NWs and 3D CoO@MnO_2 core-shell nanohybrid at 1 A g^{-1}.

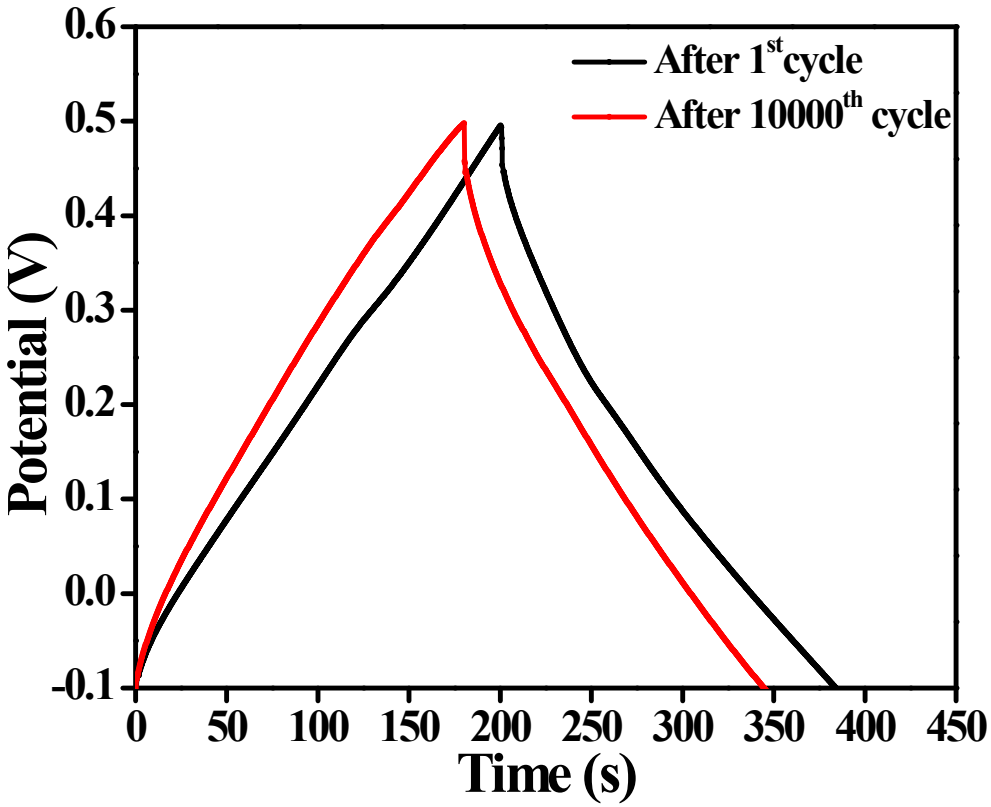

Fig. S9 GCD curves of 3D CoO@MnO_2 core-shell nanohybrid at 5 A g^{-1} (before and after stability).

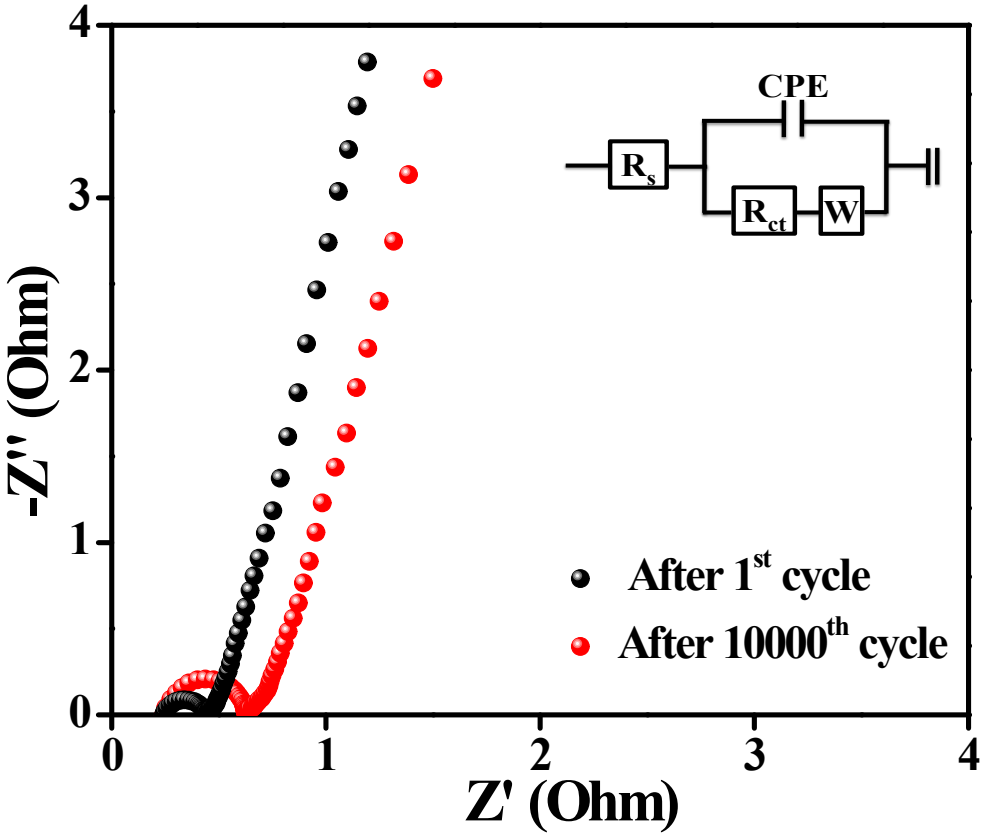

Fig. S10 EIS spectrum of 3D CoO@MnO_2 core-shell nanohybrid before and after stability tests.

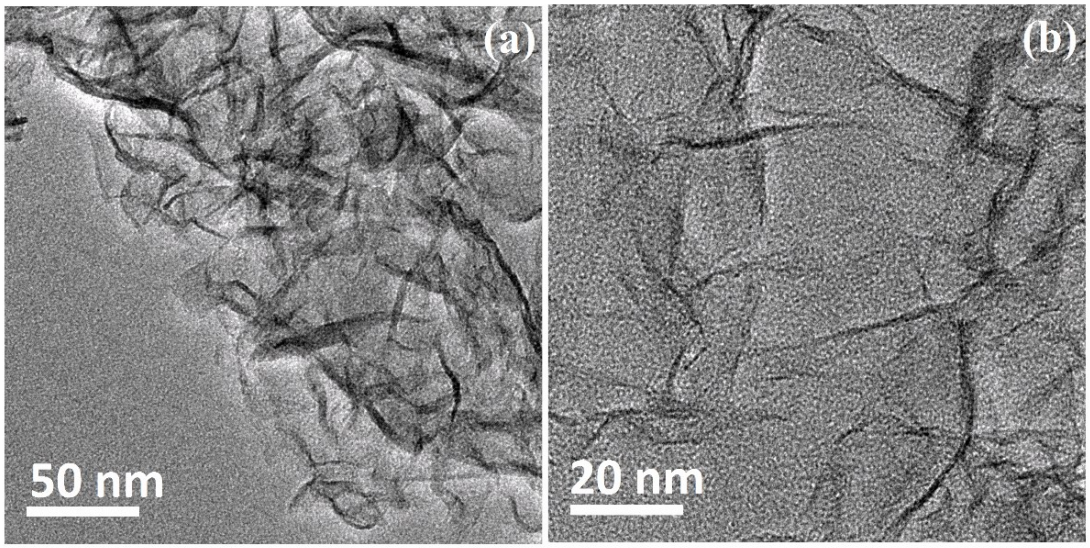

Fig. S11 TEM images with different magnification of as-synthesized NG.

The NG shows that the continuous, transparent, and crumpled graphene sheets were stacked together and formed a few-layered structure, which was perhaps initiated by N-atoms doped into graphene matrices. Also, it can be seen from the images that the physical structure and nature of NG sheets are not strongly affected during the current synthesis method.

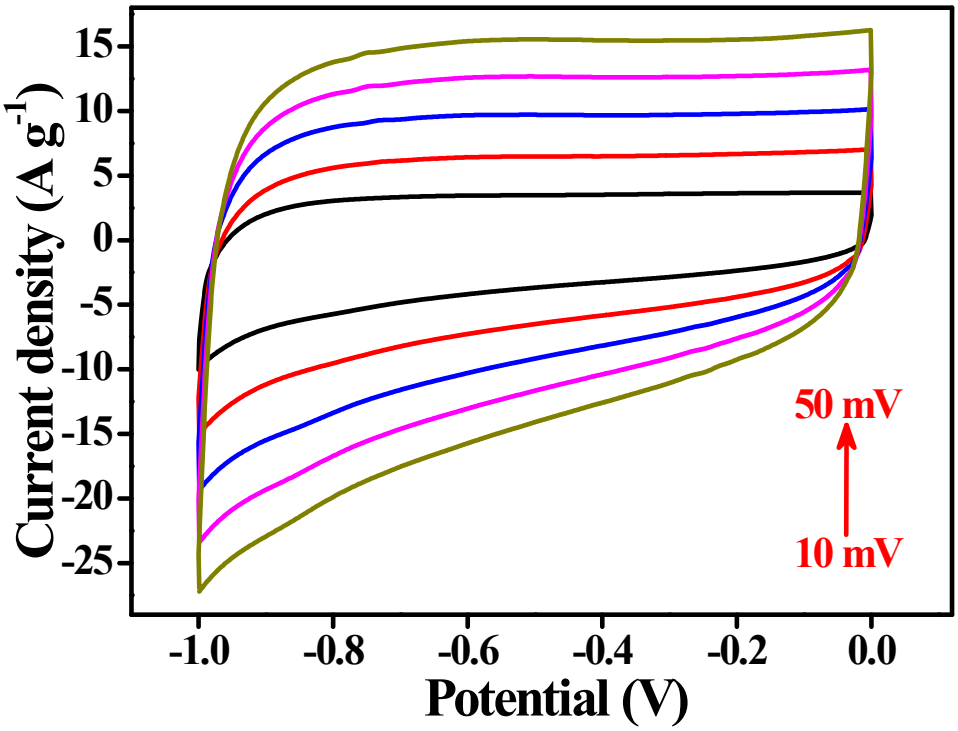

Fig. S12 CV curves of NG at different scan rates.

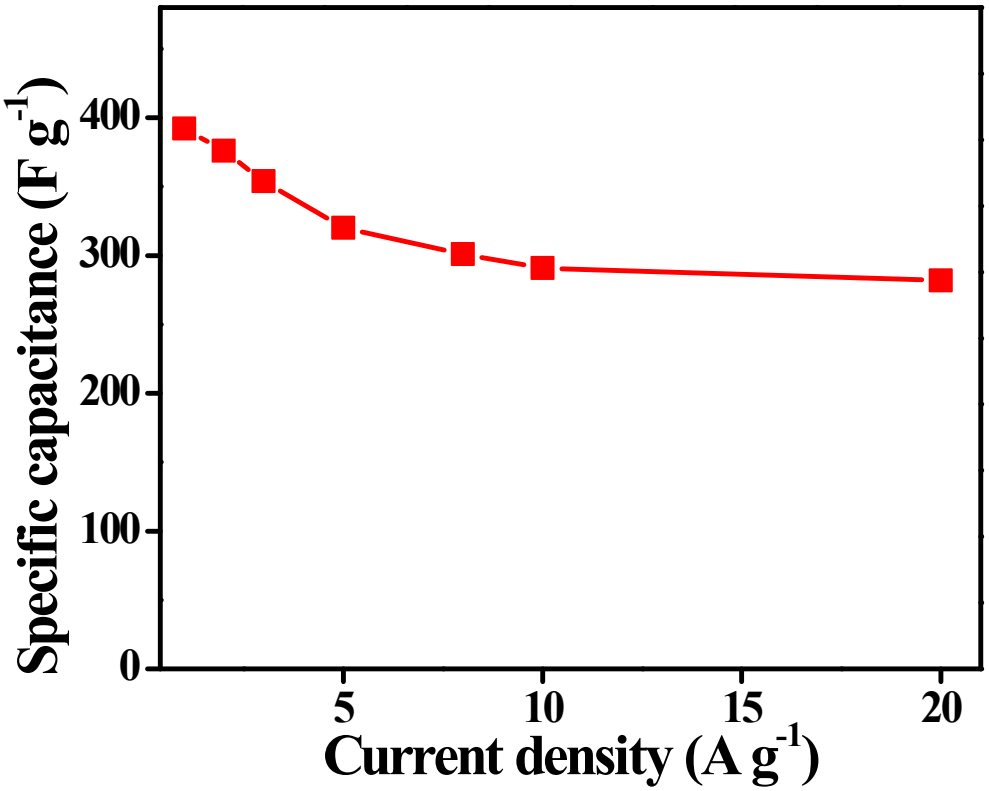

Fig. S13 Specific capacitance vs the current density of as-synthesized NG (three-electrode system).

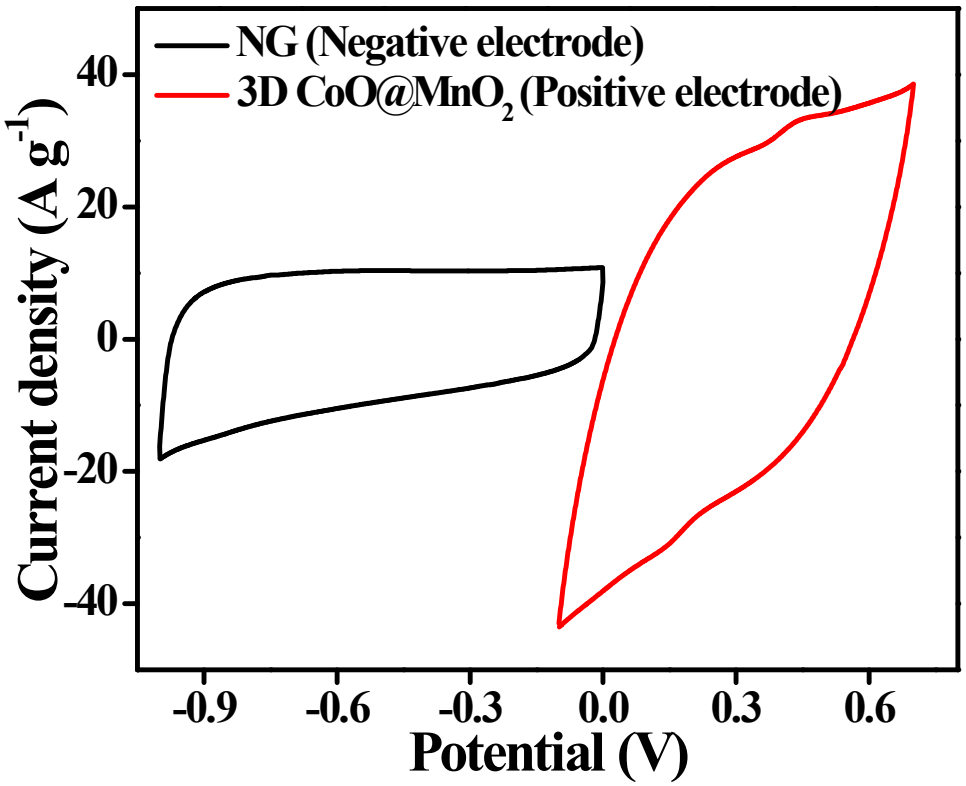

Fig. S14 3D $CoO@MnO_2$ core-shell nanohybrid and NG measured at the scan rate of 50 mVs^{-1} in a three electrode system.

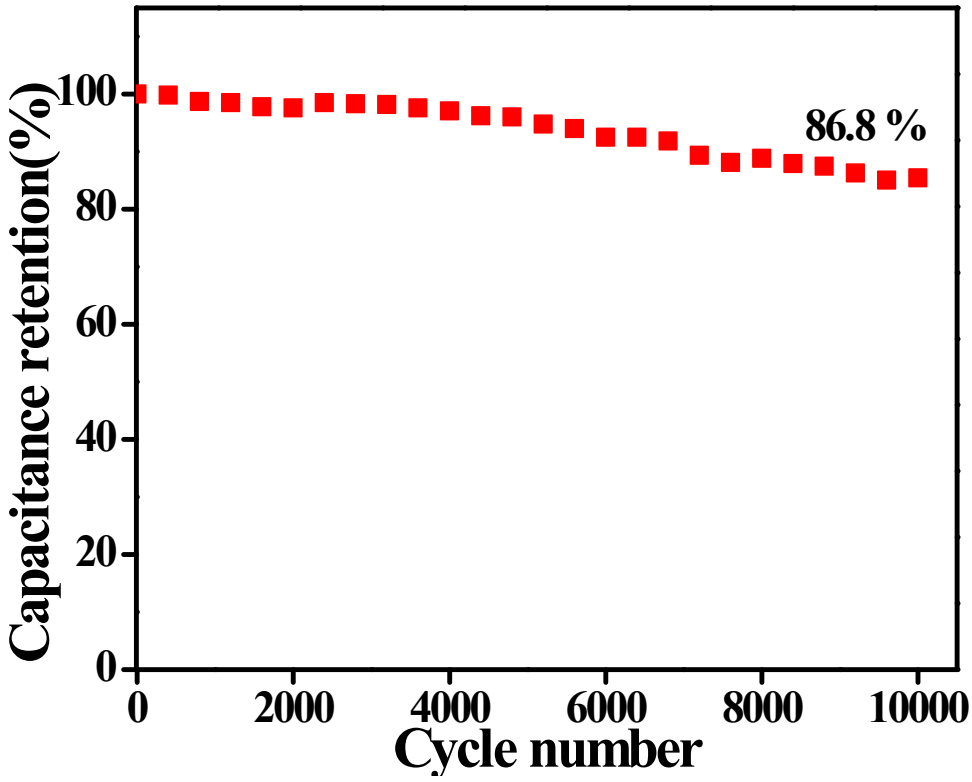

Fig. S15 The cycling stability of 3D core-shell CoO@MnO_2 //NG ASC measured at a current density of 10 A g^{-1} up to 10000 cycles test.

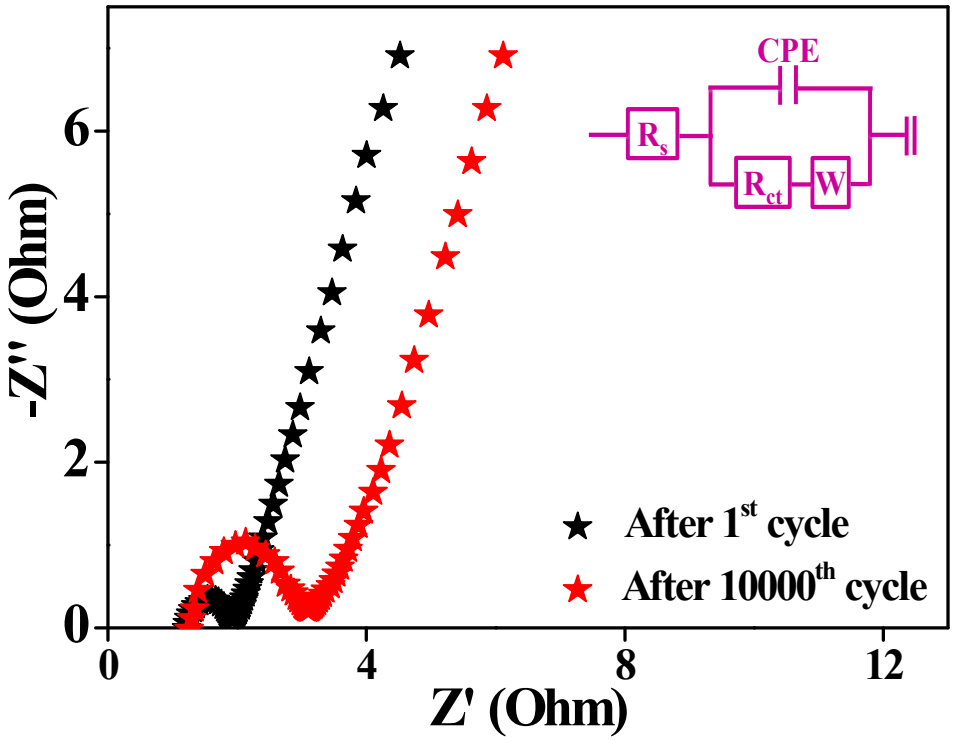

Fig. S16 EIS comparison before and after stability test of 3D core-shell CoO@MnO_2//NG ASC.

Table S1. Electrode properties comparison with reported literatures.

Reported Electrode Materials	Electrolyte	Voltage window (V)	Current density (A g^{-1})	Mass Loading (mg cm^{-2})	C_{sp} (F g^{-1})	Stability (Cycle No.)	Reference No.
α-MnO_2 NWs@δ-MnO_2 core-shell	6 M KOH	-0.1-0.55	1	$m_{hybrid} \approx 1.5$	231	98.1% 10000	1
Co_3O_4@NiO NWs	2 M KOH	0-0.55	2	$m_{Co3O4} \approx 2.1$ $m_{NiO} \approx 0.9$	853	95.1% 6000	2
ZnO@Co_3O_4	2 M KOH	0-0.52	1	$m_{Co3O4} \approx 1.5$ $m_{hybrid} \approx 2.0$	858	128.7% 6000	3
Ni@$NiCo_2O_4$	6 M KOH	0-0.45	1	$m_{hybrid} \approx 1.54$	899	93.2% 6000	4
$NiCo_2O_4$@PANI core-shell	1 M H_2SO_4	0-0.8	1	$m_{hybrid} \approx 0.89$	901	91% 3000	5
Co_3O_4@CeO_2	2 M KOH	0-0.45	2.08	$m_{Co3O4} \approx 3.0$ $m_{hybrid} \approx 4.8$	1038	94.4% 5000	6
Co_3O_4@$CoMoO_4$	3 M KOH	0-0.6	1	—	1040	87.55% 5000	7
Co_3O_4@$Co(OH)_2$ core-shell	2 M KOH	0-0.4	1	$m_{Co3O4} \approx 1.2$ $m_{Co(OH)2} \approx 0.3$	1095	92% 2000	8
$NiCo_2O_4$@3D graphene	6 M KOH	0-0.5	1	—	1402	76.6% 5000	9
SnO_2@$Ni(OH)_2$ core-shell	6 M KOH	0-0.5	0.5	—	1553	—	10
Co_3O_4@MnO_2	1 M LiOH	0-0.5	1	$m_{Co3O4} \approx$	1693	89.8%	11

Nanoeedle Arrays				1.0		5000	
3D core-shell CoO@MnO_2	6 M KOH	-0.1-0.5	1	$m_{MnO2} \approx 0.67$ $m_{CoO} \approx 1.24$ $m_{hybrid} \approx 2.13$	1835	97.7% 10000	This work

Table S2. ASC Device properties comparison with reported literatures.

Reported ASC Device	**Electrolyte**	**Device Window (V)**	**Energy Density (Wh kg^{-1})**	**Power Density (kW kg^{-1})**	**Stability (Cycle No.)**	**Reference No.**
GNR//GNR-MnO_2	PAAK-KCl	0-2	29.4	12.1	88% 5000	12
H-TiO_2@MnO_2// H-TiO_2@C core-shell	PVA-LiCl	0-1.8	59	0.045	91.2% 5000	13
MnO_2/Carbon fiber// Graphene/Carbon fiber	PVA-LiCl	0-1.5	27.2	0.98	95.2% 3000	14
V_2O_5/Pin//rGO	PVA-$LiNO_3$	0-1.8	38.7	0.9	91.1% 5000	15
RuO_2-IL-CMG// IL-CMG	PVA-H_2SO_4	0-1.8	19.7	0.5	79.4% 2000	16
$NiCo_2O_4$/CC//PGP	PVA-LiOH	0-1.8	60.9	0.57	96.8% 5000	17
β-$Ni(OH)_2$//AC	PVA-KOH	0-1.4	9.8	0.15	76% 2000	18
NiO//α-Fe_2O_3	PVA-KOH	0-1.25	12.4	0.95	85% 10000	19

Carbon aerogel // Co_3O_4 NWs	PVA-KOH	0-1.5	17.9	0.75	85% 1000	20
CoO@MnO_2//NG	PVA-KOH	0-1.8	85.9	0.85	86.8% 10000	This work

Notes and References

1 Z. P. Ma, G. J. Shao, Y. Q. Fan, G. L. Wang, J. J. Song and D. J. Shen, *ACS Appl. Mater. Interfaces*, 2016, **8**, 9050-9058.

2 X. H. Xia, J. P. Tu, Y. Q. Zhang, X. L. Wang, C. D. Gu, X. B. Zhao and H. J. Fan, *ACS Nano*, 2012, **6**, 5531-5538.

3 D. P. Cai, H. Huang, D. D. Wang, B. Liu, L. L. Wang, Y. Liu, Q. H. Li and T. H. Wang, *ACS Appl. Mater. Interfaces*, 2014, **6**, 15905-15912.

4 G. X. Gao, H. B. Wu, S. J. Ding, L. M. Liu and X. W. Lou, *Small*, 2015, **11**, 804-808.

5 N. Jabeen, Q. Y. Xia, M. Yang and H. Xia, *ACS Appl. Mater. Interfaces*, 2016, **8**, 6093-6100.

6 J. W. Cui, X. Y. Zhang, L. Tong, J. B. Luo, Y. Wang, Y. Zhang, K. Xie and Y. C. Wu, *J. Mater. Chem. A*, 2015, **3**, 10425-10431.

7 Z. X. Gu, R. F. Wang, H. H. Nan, B. Y. Geng and X. J. Zhang, *J. Mater. Chem. A*, 2015, **3**, 14578-14584.

8 X. H. Xia, J. P. Tu, Y. Q. Zhang, J. Chen, X. L. Wang, C. D. Gu, C. Guan, J. S. Luo and H. J. Fan, *Chem. Mater.*, 2012, **24**, 3793-3799.

9 C. F. Zhang, T. Kuila, N. H. Kim, S. H. Lee and J. H. Lee, *Carbon*, 2015, **89**, 328-339.

10 Q. Q. Ke, C. Guan, M. R. Zheng, Y. T. Hu, K. H. Hoa and J. Wang, *J. Mater. Chem. A*,

2015, **3**, 9538-9542.

11 D. Z. Kong, J. S. Luo, Y. L. Wang, W. N. Ren, T. Yu, Y. S. Luo, Y. P. Yang and C. W. Cheng, *Adv. Funct. Mater.*, 2014, **24**, 3815-3826.

12 M. K. Liu, W. W. Tjiu, J. S. Pan, C. Zhang, W. Gao and T. X. Liu, *Nanoscale*, 2014, **6**, 4233-4242.

13 X. H. Lu, M. H. Yu, G. M. Wang, T. Zhai, S. L. Xie, Y. C. Ling, Y. X. Tong and Y. Li, *Adv. Mater.*, 2013, **25**, 267-272.

14 N. Yu, H. Yin, W. Zhang, Y. Liu, Z. Y. Tang and M. Q. Zhu, *Adv. Energy Mater.*, 2016, **6**, 1501458.

15 X. Zhou, Q. Chen, A. Q. Wang, J. Xu, S. S. Wu and J. Shen, *ACS Appl. Mater. Interfaces*, 2016, **8**, 3776-3783.

16 B. G. Choi, S. J. Chang, H. W. Kang, C. P. Park, H. J. Kim, W. H. Hong, S. G. Lee and Y. S. Huh, *Nanoscale*, 2012, **4**, 4983-4988.

17 Z. Gao, W. L.Yang, J. Wang, N. N. Song and X. D. Li, *Nano Energy*, 2015, **13**, 306-317.

18 S. T. Senthilkumar and R. K. Selvan, *Phys. Chem. Chem. Phys.*, 2014, **16**, 15692-15698.

19 S. W. Zhang, B. Yin, Z. B. Wang and F. Peter, *Chemical Engineering Journal*, 2016, **306**, 193-203.

20 W. W. Liu, X. Li, M. H. Zhu and X. He, *J. Power Sources*, 2015, **282**, 179-186.